

## Supporting information

### **Engineering $\text{Co}_3\text{O}_4@3\text{DOM LaCoO}_3$ multistage-pore nanoreactor with superior $\text{SO}_2$ resistance for toluene catalytic combustion**

Zhan Shi<sup>a, b</sup>, Fang Dong<sup>b</sup>, Weiliang Han<sup>b</sup>, Xiuyan Dong<sup>a\*</sup>, Zhicheng Tang<sup>b\*</sup>

*(a. School of Chemistry and Chemical Engineering, Lanzhou Jiaotong University,  
Lanzhou 730070, China.*

*b. State Key Laboratory for Oxo Synthesis and Selective Oxidation, and National  
Engineering Research Center for Fine Petrochemical Intermediates, Lanzhou  
Institute of Chemical Physics, Chinese Academy of Sciences, Lanzhou, 730000,  
China.)*

---

\*Corresponding author.

E-mail address: [dongxy@mail.lzjtu.cn](mailto:dongxy@mail.lzjtu.cn) (X. Dong), [tangzhicheng@licp.cas.cn](mailto:tangzhicheng@licp.cas.cn) (Z. Tang)

## 1. Catalyst characterizations

The morphology of the catalyst samples was analyzed by transmission electron microscopy (TEM, JEOL-JEM-2010). Scanning electron microscope (SEM) images of the samples were obtained by a JSM-6701F cold field emission scanning electron microscope. The crystal phases of each element in the catalyst were determined by an X-ray diffraction instrument (XRD, Japan Smartlabse) (scanning angle of  $10^{\circ}$ - $90^{\circ}$ , scanning speed of  $0.5^{\circ}/\text{min}$ , 60 kV, 55 mA) under the radiation of  $\lambda=1.5406$  nm. The Fourier transform infrared spectroscopy (FTIR) analysis of the samples was performed using a Fourier infrared spectrometer (Nexus 870, Nicolet), and ATR technology was used for FTIR analysis. Brunauer-Emmett-Teller (BET) surface area, the pore size, and the pore volume of the catalysts were obtained by adsorption and desorption of nitrogen in the ASAP 2020 instrument (America Micromeritics). The real content of each metal on the catalyst was obtained by measuring each catalyst with an Agilent ICP-OES 730 instrument. Infrared spectra were tested with a Nicolet Nexus 870 Fourier transform infrared spectrometer. X-ray photoelectron spectroscopy (XPS) measurements were performed with a Thermo Scientific 250 Xi.

The multifunctional dynamic adsorption instrument TP-5080-D was used to analyze the acidity and redox capacity of the catalyst surface. For  $\text{H}_2$ -TPR, a 50 mg sample was heated from room temperature to  $900^{\circ}\text{C}$  in reduced gas with volume fractions of 5 vol %  $\text{H}_2$  and 95 vol %  $\text{N}_2$ , and the detector signal was continuously recorded. For the  $\text{O}_2$ -TPD test, the catalyst (50 mg) was pretreated with nitrogen (99.9%) for 1 h at  $300^{\circ}\text{C}$ . When the temperature dropped to  $50^{\circ}\text{C}$ , the  $\text{O}_2$  (5%  $\text{O}_2/\text{N}_2$ )

adsorption was carried out for 60 min. After the adsorption was over, purged for 0.5 h, and the desorbed O<sub>2</sub> signal was detected at 50-900 °C. The temperature-programmed desorption operation of NH<sub>3</sub>-TPD, SO<sub>2</sub>-TPD and Toluene-TPSR was similar to that of O<sub>2</sub>-TPD, except that O<sub>2</sub> was changed to NH<sub>3</sub>, SO<sub>2</sub> and Toluene.

## 2. Catalytic activity measurements

The activity and stability of the catalysts were tested with the help of Toluene (C<sub>7</sub>H<sub>8</sub>) as a probe molecule, which was essential for the study of the catalytic oxidation performance of VOCs. The catalytic oxidation of toluene was evaluated by using a fixed-bed flow reactor operating at steady-state flow mode. Then, 0.4 g catalysts (40–60 mesh) and 0.7 g quartz sand (40–60 mesh) were mixed uniformly. They were put onto the reactor. The reaction gas containing VOCs (3000 ppm) was generated by bubbling air through a VOC saturator, and then passed through the reactor with a weight hourly space velocity (WHSV) of 30000 ml g<sup>-1</sup> h<sup>-1</sup>. The first temperature was 100 °C. The activity was measured per 20 °C. Before each test, it needed to stabilize for 1 h. Reactants and products were analyzed with an online GC-6820 gas chromatograph with a flame ionization detector, Conversion was defined as. The conversion efficiency of C<sub>7</sub>H<sub>8</sub> was calculated by the following equation:

$$x = \frac{C_{in} - C_{out}}{C_{in}} \times 100\%$$

Where x is the conversion of C<sub>7</sub>H<sub>8</sub>, C<sub>in</sub> and C<sub>out</sub> are the inlet and outlet concentrations of C<sub>7</sub>H<sub>8</sub> in the gas phase.

## 3. In-situ FTIR measurement

In-situ diffuse reflectance infrared Fourier transform spectroscopy (DRIFTS) spectra was collected with VERTEX 70 spectrometer equipped with an MCT detector and a CaF<sub>2</sub> window in-situ cell. DRIFTS cell was used as the reaction chamber and the spectra were collected in the frequency range of 4000-600 cm<sup>-1</sup>. 200 mg grain catalyst (40-60 mesh) was packed in DRIFTS cell. For C<sub>7</sub>H<sub>8</sub> adsorption spectra, the Co<sub>3</sub>O<sub>4</sub>@LaCoO<sub>3</sub> catalysts were pretreated at 300 °C by flowing Ar for 30 min. After the temperature cooled to 50 °C, it was exposed to 15 ppm C<sub>7</sub>H<sub>8</sub>/Ar feed at a flow rate of 25 mL/min, and the adsorption was saturated. Subsequently, the adsorption saturation was reached at different temperatures (50 °C, 100 °C, 150 °C, 200 °C, 250 °C, 300 °C, 350 °C and 400 °C). For the oxidation of C<sub>7</sub>H<sub>8</sub>, the Co<sub>3</sub>O<sub>4</sub>@LaCoO<sub>3</sub> catalysts were treated with air, and then the 15 ppm C<sub>7</sub>H<sub>8</sub> in Ar was pre-adsorbed on the clean samples at 50 °C for 30 min. Subsequently, the air with a flow of 25 mL/min was poured and the in-situ DRIFTS spectra were collected at different temperature with a heating rate of 10 °C/min.

#### 4. Kinetic studies

The catalytic performance could also be identified by kinetic studies, such as apparent activation energy ( $E_a$ ), which was measured as follows:

$$\ln r = \frac{-E_a}{RT} + C \quad (1)$$

In equation (1),  $r$  represented the reaction rate (mol·s<sup>-1</sup>),  $T$  referred to the reaction temperatures, and  $C$  was a constant term.

$$r = \frac{F \times X_{toluene}}{W} \quad (2)$$

In equation (2),  $X_{\text{toluene}}$  denoted the conversion of toluene,  $F$  indicated the feeding rate ( $\text{mol}\cdot\text{s}^{-1}$ ), and  $W$  corresponded to the mass of the catalyst. Therefore, the plots of  $\ln r$  and  $1000/T$  yielded the  $E_a$  value.

The kinetic studies also included specific reaction rates, such as the catalyst's mass ( $R_m$ ), which was calculated required the following equation:

$$R_m = \frac{F \times \eta_{\text{toluene}}}{W} \quad (3)$$

$$\eta_{\text{toluene}} = \log \frac{1}{1 - \frac{X_{\text{toluene}}}{100}} \quad (4)$$

Turnover frequency (TOF), defined as the number of toluene molecules converted per active site per second, is calculated according to the equation:

$$\text{TOF} = \frac{F_{\text{toluene}} * X_{\text{toluene}}}{\frac{(x(\text{Co}^{3+}) * x(\text{Co}))}{M_{\text{Cat}}} * m_{\text{Cat}}} \quad (5)$$

Where  $F_{\text{toluene}}$  is the propane flow rate ( $\text{mol/s}$ ),  $X_{\text{toluene}}$  is the conversion of toluene,  $m_{\text{cat}}$  is the mass of the catalyst ( $\text{g}$ ),  $M_{\text{Cat}}$  ( $\text{g}$ ) is the molar of the catalysts,  $x(\text{Co}^{3+})$  are the ratios of  $\text{Co}^{3+}/\text{Co}_{\text{total}}$ , respectively;  $x(\text{Co})$  is the total contents of Co in various samples (obtained by XPS experiments).

**Table S1**

Comparison of catalysts reported in the literature for catalytic oxidation of toluene with this work.

Catalysts	T <sub>50</sub> (°C)	T <sub>90</sub> (°C)	Concentration (ppm)	GHSV mL (g·h) <sup>-1</sup>	Ref.
La <sub>0.5</sub> Sr <sub>0.5</sub> Co <sub>0.8</sub> Fe <sub>0.2</sub> O <sub>3</sub>	251	270	1000	30000	[1]
La <sub>0.9</sub> FeO <sub>3</sub>	287	310	1000	20000	[2]
SmMnO <sub>3</sub>	255	313	1000	32000	[3]
Co <sub>3</sub> O <sub>4</sub> /SiO <sub>2</sub> -WI	286	305	3000	30000	[4]
6.4Au/bulk Co <sub>3</sub> O <sub>4</sub>	244	277	1000	20000	[5]
Co <sub>3</sub> O <sub>4</sub>	266	285	1000	20000	[6]
LaCoO <sub>3</sub>	290	331	1000	30000	[7]
LaCoO <sub>3</sub> @Co <sub>3</sub> O <sub>4</sub>	249	265	3000	30000	This work
Co <sub>3</sub> O <sub>4</sub> @LaCoO <sub>3</sub>	229	254	3000	30000	This work

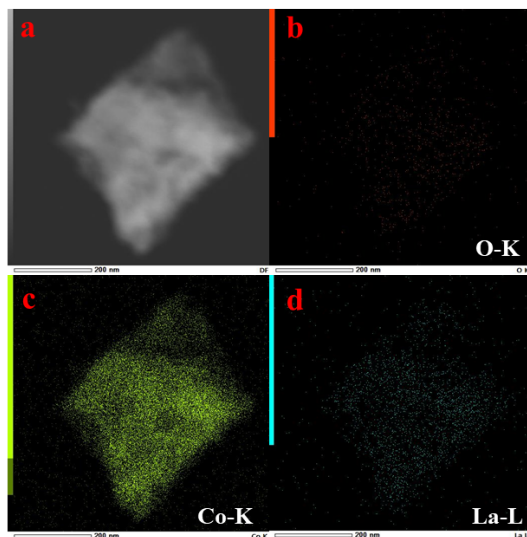


**Fig. S1.** Mapping analysis of  $\text{LaCoO}_3@ \text{Co}_3\text{O}_4$  catalyst.

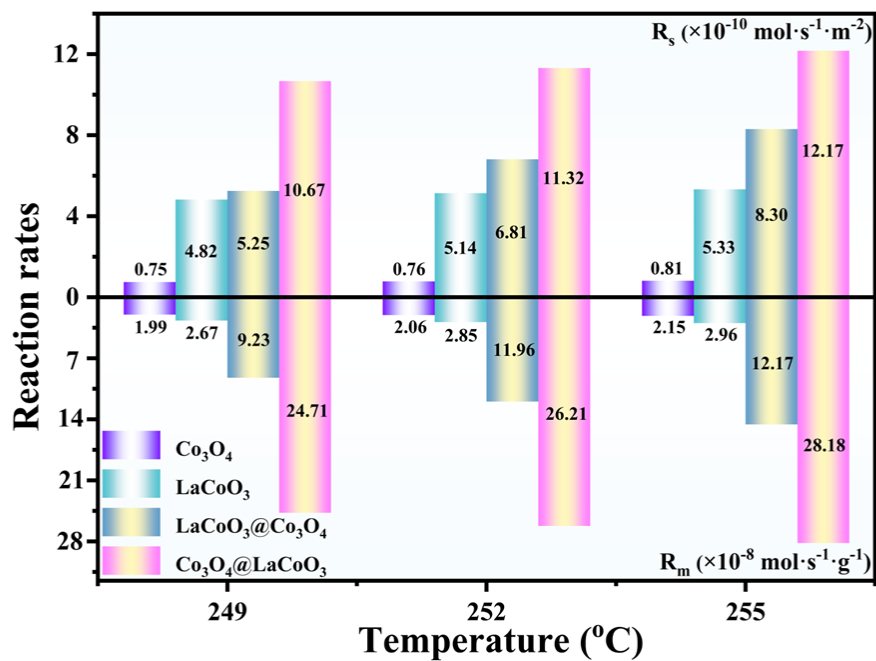


Fig. S2.  $R_s$  (reaction rates based on the specific area) and  $R_m$  (reaction rates based on the catalyst mass) of catalysts.



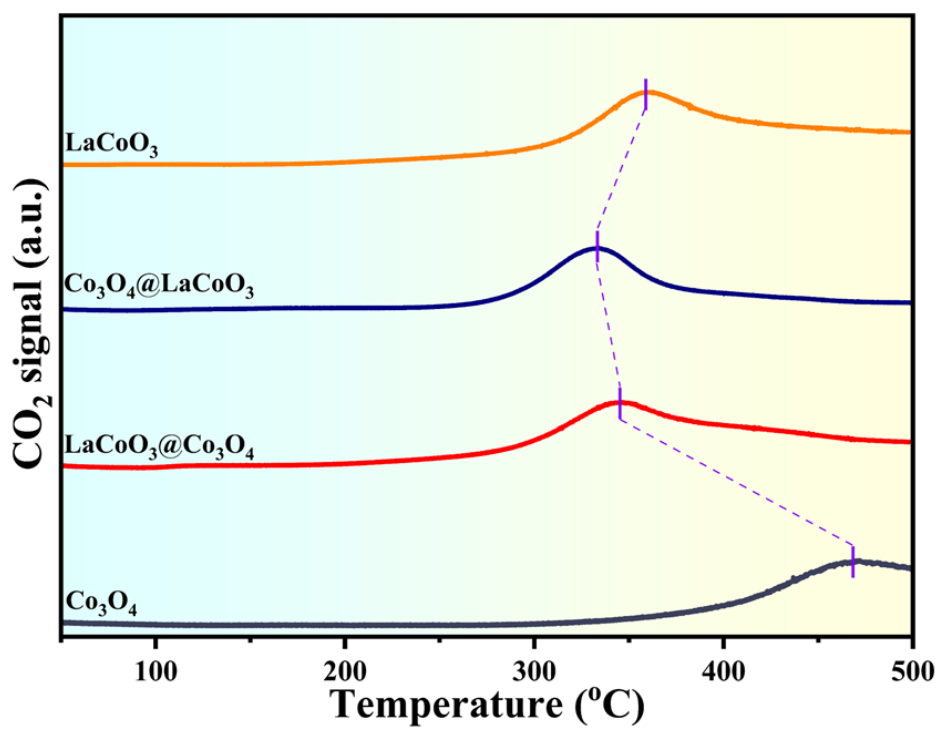
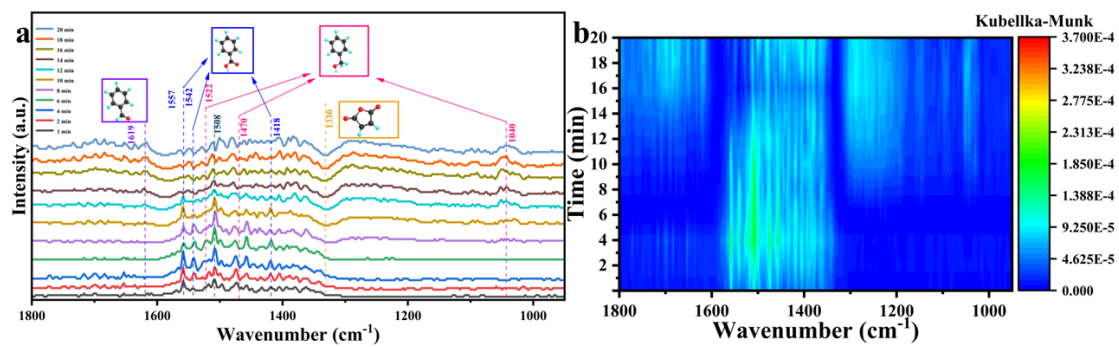


Fig. S3. Toluene-TPSR profiles.



**Fig. S4.** In-situ DRIFT spectra for adsorption of the  $\text{Co}_3\text{O}_4@\text{LaCoO}_3$  catalyst exposure to 15 ppm toluene at different time.

## References

- [1] Y. Li, S. Liu, K. Yin, D. Jia, Y. Sun, X. Zhang, J. Yan, L. Yang, Understanding the mechanisms of catalytic enhancement of La-Sr-Co-Fe-O perovskite-type oxides for efficient toluene combustion, *J. Environ. Chem. Eng.* 11 (2023) 109050.
- [2] M. Wu, S. Chen, W. Xiang, Oxygen vacancy induced performance enhancement of toluene catalytic oxidation using LaFeO<sub>3</sub> perovskite oxides, *Chem. Eng. J.* 387 (2020) 124101.
- [3] L. Liu, J. Sun, J. Ding, Y. Zhang, J. Jia, T. Sun, Catalytic Oxidation of VOCs over SmMnO<sub>3</sub> Perovskites: Catalyst Synthesis, Change Mechanism of Active Species, and Degradation Path of Toluene, *Inorg. Chem.* 58 (2019) 14275–14283.
- [4] Y. Xi, F. Dong, Z. Ji, Z. Tang, J. Zhang, Design order macro-meso porous structure monolithic Co<sub>3</sub>O<sub>4</sub>/SiO<sub>2</sub> catalyst via a novel 3D printing for the highly efficient catalytic combustion of toluene, *J. Clean. Prod.* 379 (2022) 134694.
- [5] Y. Liu, H. Dai, J. Deng, S. Xie, H. Yang, W. Tan, W. Han, Y. Jiang, G. Guo, Mesoporous Co<sub>3</sub>O<sub>4</sub>-supported gold nanocatalysts: Highly active for the oxidation of carbon monoxide, benzene, toluene, and o-xylene, *J. Catal.* 309 (2014) 408–418.
- [6] H. Yang, H. Dai, J. Deng, S. Xie, W. Han, W. Tan, Y. Jiang, C.T. Au, Porous Cube-Aggregated Co<sub>3</sub>O<sub>4</sub> Microsphere-Supported Gold Nanoparticles for Oxidation of Carbon Monoxide and Toluene, *ChemSusChem* 7 (2014) 1745–1754.
- [7] H. Chen, G. Wei, X. Liang, P. Liu, H. He, Y. Xi, J. Zhu, The distinct effects of

substitution and deposition of Ag in perovskite  $\text{LaCoO}_3$  on the thermally catalytic oxidation of toluene, *Appl. Surf. Sci.* 489 (2019) 905–912.